# Frequency, intensity, and sensitivity to sea surface temperature of North Atlantic tropical cyclones in best-track and simulated data

Sarah Strazzo,[1] James B. Elsner,[1] Jill C. Trepanier,[2] and Kerry A. Emanuel[3]

Received 9 May 2013; accepted 10 June 2013.

[1] Synthetic hurricane track data generated from a downscaling approach are compared to best-track (observed) data to analyze differences in regional frequency, intensity, and sensitivity of limiting intensity to sea surface temperature (SST). Overall, the spatial distributions of observed and simulated hurricane counts match well, although there are relatively fewer synthetic storms in the eastern quarter of the basin. Additionally, regions of intense synthetic hurricanes tend to coincide with regions of intense observed hurricanes. The sensitivity of limiting hurricane intensity to SST computed from synthetic data is slightly lower than sensitivity computed from observed data ($5.5 \pm 1.31$ m s$^{-1}$ (standard error, SE) and $8.6 \pm 1.57$ m s$^{-1}$ (SE), respectively); however, the synthetic data produce sensitivity values that are much closer to the observed values than those obtained from two global climate models (GCMs) in a previous study. Despite a close match in the magnitude of basin wide sensitivities, the spatial variability of sensitivities do not match. These values tend to be highest in the western portion of the basin for the observed data, while the opposite is true for the synthetic data.

**Citation:** Strazzo, S., J. B. Elsner, J. C. Trepanier, and K. A. Emanuel (2013), Frequency, intensity, and sensitivity to sea surface temperature of North Atlantic tropical cyclones in best-track and simulated data, *J. Adv. Model. Earth Syst.*, *5*, doi:10.1002/jame.20036.

## 1. Introduction

[2] Throughout the past century, tropical cyclones (TCs) have caused considerable damage to both human life and property. As global climate change continues to be an area of concern and significant scientific inquiry, many question how TC frequencies and intensities may be affected by a warming climate [e.g., *Emanuel*, 2005; *Elsner et al.*, 2008; *Vecchi et al.*, 2008; *Knutson et al.*, 2010]. In recent years, several methods for addressing questions about TCs and climate change have emerged. One such method employs statistical models built on observational hurricane data [e.g., *Mann and Emanuel*, 2006; *Elsner et al.*, 2008; *Kossin et al.*, 2010]. These models yield insight into the current state while also providing evidence for potential future changes. Despite these benefits, uncertainty associated with statistical model parameters is large owing to short, heterogeneous data records [e.g., *Landsea et al.*, 2004].

[3] In addition to statistical models, global climate models (GCMs) have been proposed as potentially useful tools for studying tropical cyclone climate [e.g., *Broccoli and Manabe*, 1990; *Bengtsson et al.*, 1996]. In fact, recent model analyses demonstrated that some GCMs are capable of reproducing aspects of the observed TC climatology [e.g., *Camargo et al.*, 2005; *Oouchi et al.*, 2006; *LaRow et al.*, 2008; *Zhao et al.*, 2009; *Strazzo et al.*, 2013]. Models with horizontal grid spacing as low as 20 km have been employed to examine TC frequencies and intensities under various global warming scenarios [e.g., *Oouchi et al.*, 2006; *Murakami et al.*, 2011]. However, despite some promising results, hurricane eyewall structure is still not adequately resolved [*Chen et al.*, 2007]. Because of this limitation, caution must be exercised when interpreting model results, particularly with respect to TC intensity.

[4] Another method for assessing tropical cyclone climate has recently been added to the repertoire. This technique makes use of the National Center for Environmental Prediction/National Center for Atmospheric Research (NCEP/NCAR) reanalysis data set to generate synthetic hurricane track data [*Emanuel*, 2006]. The synthetic data consist of a series of potential tracks and intensities covering the period 1980–2010, inclusive. Synthetic TCs are generated using a random seeding method [*Emanuel et al.*, 2008], and then tracked using a separate method that employs NCEP/NCAR reanalysis data. Storm intensity along the tracks is simulated using a deterministic numerical model. Variants on this method have been applied in *Emanuel et al.* [2008] and *Emanuel* [2010]. Results from these papers indicate that

[1]Department of Geography, Florida State University, Tallahassee, Florida, USA.
[2]Department of Geography and Anthropology, Louisiana State University, Baton Rouge, Louisiana, USA.
[3]Department of Earth, Atmospheric and Planetary Science, Massachusetts Institute of Technology, Cambridge, Massachusetts, USA.


1942-2466/13/10.1002/jame.20036

tracks generally conform to the spatial distribution and interannual variability of observed tropical cyclones over the North Atlantic basin. Additional details concerning the generation of these synthetic tracks will be discussed further in section 2.

[5] Despite recent advances, GCMs have limitations in assessing tropical cyclones in the context of climate and climate change. This is particularly true for questions concerning intensity. For example, one potential limitation of GCMs was highlighted in *Elsner et al*. [2013], who applied extreme value theory to examine the sensitivity of hurricane maximum wind speed to sea surface temperature (SST) for observations and two atmospheric GCMs. They demonstrated that while observations exhibited sensitivity values of $7.9 \pm 1.19$ m $s^{-1}$ $K^{-1}$ (SE), values for the models were as low as $1.8 \pm 0.42$ m $s^{-1}$ $K^{-1}$ (SE).

[6] Although this method has been applied to GCM-generated track data, it has not yet been applied to examine sensitivity values for synthetic track data generated through the downscaling methods outlined in *Emanuel* [2006]. From the *Elsner et al*. [2013] results, we know that the current suite of GCMs is unable to accurately capture the sensitivity of the most intense hurricanes to SST. These results agree well with the known limitations of GCMs to realistically simulate eyewall structure and maximum wind speed. However, we do not know how well the synthetic track data match observations with respect to sensitivity of limiting intensity to SST. As the downscaling approach continues to be utilized for hurricane-climate research, it also may be useful to examine sensitivity values for the synthetic track data. Because the downscaling approach incorporates a high-resolution deterministic model capable of resolving the eyewall region of the hurricane, we hypothesize that the synthetic hurricanes will better match the observed sensitivity of limiting intensity to SST.

[7] This study provides a comparison of the observational and synthetic hurricane data sets using metrics of frequency, intensity, and the sensitivity of intensity to SST. We apply a statistical model similar to that introduced in *Elsner et al*. [2012b] and later applied to GCM-generated track data in *Elsner et al*. [2013]. To avoid some of the assumptions that are necessary to estimate the statistical model, we also calculate the sensitivity values using a simplified method (discussed in detail in section 4). The paper is organized as follows: the data are discussed in section 2, the spatial methodology is introduced in section 3, relationships between SST and TC frequency and intensity are presented in section 4, and the spatial variability of these relationships are presented in section 5. Finally, section 6 summarizes the results and provides some concluding remarks.

## 2. Data

[8] This study compares simulated TC data with best-track data over the entire North Atlantic basin for the period 1980–2010. For observations we utilize the hurricane data (HURDAT) best-track data set maintained by the U.S. National Oceanic and Atmospheric Administration (NOAA) National Hurricane Center (NHC). The best-track data set contains the 6 hourly center locations and intensities of all known tropical cyclones across the North Atlantic basin, including the Gulf of Mexico and Caribbean Sea. Center locations (center fixes) are given in geographic coordinates (in tenths of degrees); intensities, representing the 1 min near-surface 10 m wind speeds, are given in knots; and minimum central pressures are given in millibars. The version of HURDAT used here contains cyclones over the period 1851–2010, inclusive http://www.nhc.noaa.gov/pastall.shtml. Information on the history and origin of these data is available from *Jarvinen et al*. [1984].

[9] As in *Elsner et al*. [2012b] and *Elsner et al*. [2013], we use a technique combining splines and spherical geometry to interpolate the raw 6 hourly best-track data to hourly intervals. The resulting interpolated best-track data set contains hourly estimates of TC positions, minimum central pressures, and maximum wind speeds. Details of the procedure, including R code for the interpolation, are given in *Elsner and Jagger* [2013]. When the synthetic data were generated, TCs with peak lifetime wind speeds of less than 40 knots were not included. Thus, we also remove any observed TCs with lifetime maximum wind speeds of less than 40 knots (31 TCs out of a total of 364). Next, 60% of the forward speed is subtracted from the best-track speed to obtain an estimate of the cyclone's maximum rotational velocity [*Emanuel et al*., 2006]. We remove all points over land so that only TCs over water are included in the analysis.

[10] The simulated (synthetic) data represent a large number of cyclone tracks together with a deterministic intensity model integrated along each track. The tracks are based on a weighted average of the upper and lower tropospheric flow plus "beta drift" [*Emanuel*, 2006, 2010]. The flow is simulated from wind time series where the monthly mean, variance, and covariances conform to the statistics derived from the NCEP/NCAR reanalysis data. Wind shear derived from the flows serves as input to the intensity model. Statistics of the simulated hurricane motion match the statistics of observed hurricane motion. Finally, the method ensures that hurricane intensity conforms broadly to the underlying physics, including the natural limitations imposed by potential intensity, ocean coupling, vertical wind shear, and landfall.

[11] We reformat the data to match the best-track format and convert the wind speeds from units of knots to meters per second. The synthetic data contain a total of 6200 tropical cyclones, which compares to 332 observed tropical cyclones over the same 1980–2010 time period. The synthetic data consist of 2 hourly simulated samples for each storm; therefore, we take only the even hours of the previously described hourly interpolated best-track data set to match the sampling frequency of the synthetic samples. Figure 1 (top) shows the distribution of the rotational component of the wind speeds for the best-track and simulated hurricane sets. With more

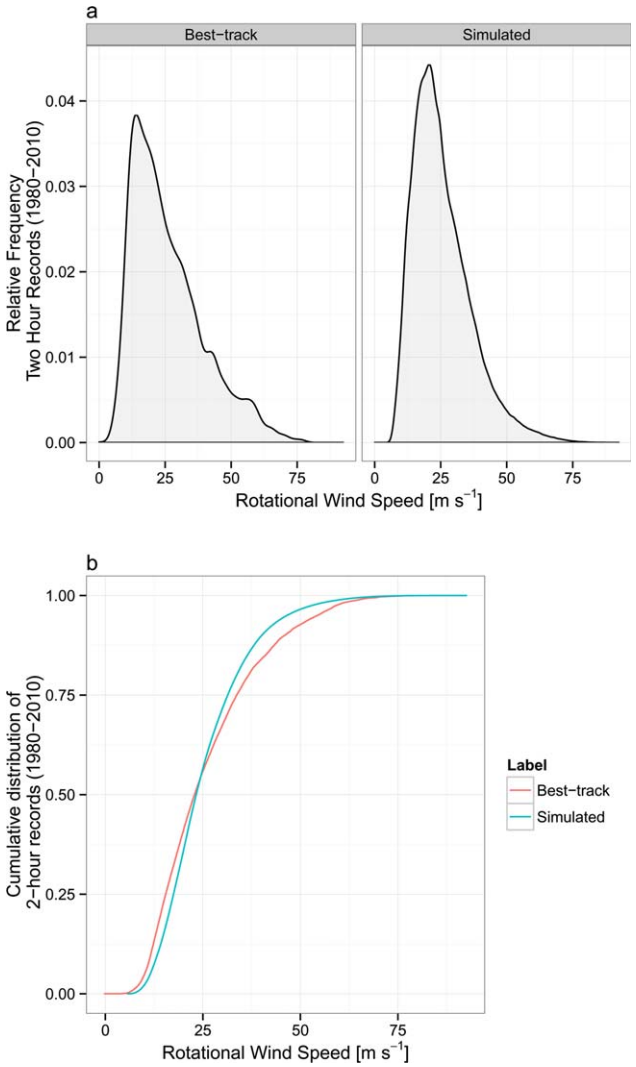


**Figure 1.** Rotational winds speeds from observed and synthetic tropical cyclones: (a) relative frequency and (b) cumulative distributions.

TCs, the synthetic distribution is smoother than the observed distribution. The cumulative distribution of observed and simulated winds is given in Figure 1 (bottom), where it can be seen that the distributions match near the 55th percentile (25 m $s^{-1}$).

[12] In addition to the observed and simulated TC track data, this study makes use of the NOAA Extended Reconstructed Sea Surface Temperature (ERSST) V3b data set to calculate sensitivity values (available from www.esrl.noaa.gov/psd/data/gridded/data.noaa.ersst.html). For each grid point, we take the average August-September-October (ASO) value over the 1980–2010 time period. The SST data are then transformed from latitude-longitude grids to a Lambert conformal conic (LCC) projection with secant latitudes of 30° and 60° N and a projection center of 60° W longitude (the same projection used by the NHC for seasonal summary maps).

## 3. Spatial Framework for Comparing Hurricane Climatology

[13] This study consists of a spatial comparison of simulated and observed hurricanes in terms of frequency, intensity, and sensitivity to SST. To accomplish this, we first create separate spatial points data frames for the observed and simulated hurricanes and transform the center fix locations given in latitude and longitude to the same LCC projection as is used to project the SST data. We next create a hexagonal tessellation of the basin from the set of best-track hurricanes. This is done by gridding a rectangular domain encompassing the set of observed hurricane locations into equal-area hexagons [*Elsner et al.*, 2012a, 2012b]. We opt to use a spatial lattice because it provides a uniform framework for comparing observed and synthetic tracks. This approach allows us to easily calculate spatial statistics while not compromising the physical interpretation. For example, we may examine the spatial distribution of TCs by summing the number of unique storms within each hexagon, which results in integer TC counts for each hexagon. Conversely, if we had instead used area-corrected latitude-longitude grids, TC counts would no longer be integer values, making their interpretation less physically meaningful. Additional details and justification for the spatial framework may be found in *Elsner et al.* [2012a].

[14] The area of each hexagon is a compromise between being large enough to have a sufficient number of hurricanes passing through to reliably estimate model parameters and being small enough that regional variations are meaningful. Here we use an area of 8.33 $\times$ $10^5$ $km^2$ (or an edge length of 567 km), which results in 31 hexagons over the basin that each covered at least 21 unique TCs over the 1980–2010 time period. Additional grids of varying sized hexagons are briefly examined in section 4. Once the hexagon tessellation is created, it is overlaid onto the best-track and simulated track points to obtain per grid hurricane counts and maximum intensities for both observations and the simulated data.

[15] We remove hexagons containing fewer than 21 observed tropical cyclones. This is done so that each hexagon has a sufficient number of wind speed values to estimate the limiting-intensity model. Within a single hexagon, the maximum number of observed TCs is 76, which compares with a maximum of 2135 simulated TCs.

[16] Figure 2 depicts the observed and simulated number of hurricanes per hexagon grid as a choropleth map. From Figure 2, it is clear that there are at least an order of magnitude more simulated hurricanes than observed hurricanes. Because of this, we instead focus on spatial patterns of TC counts for the best-track and synthetic data. Grids containing the most observed TCs occur in the south central portion of the Atlantic and east of the U.S. eastern seaboard. In contrast to observations, grids with the most simulated TCs tend to be shifted farther west in the basin with relatively fewer storms in the southeastern portion of the Atlantic.

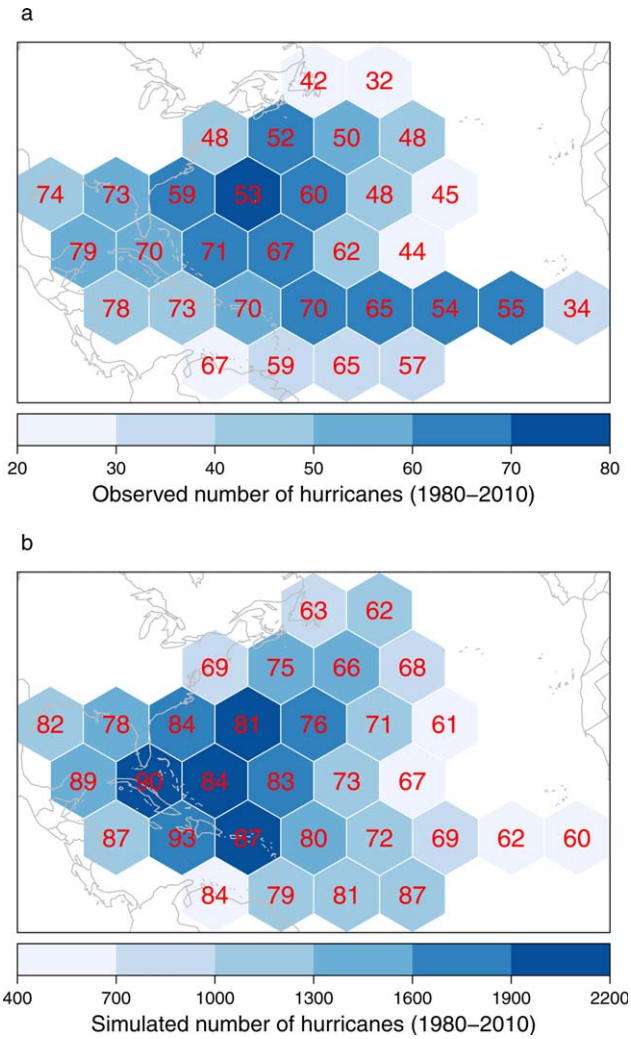


**Figure 2.** Tropical cyclone counts (color scale) and maximum intensities (red text): (a) observed data over the period 1980–2010 and (b) synthetic data. The maximum intensities are the fastest rotational wind speeds in m $s^{-1}$.

Nevertheless, the correlation between the observed and simulated counts across the domain is a fairly high +0.69.

[17] Also interesting in Figure 2 is the pattern of per grid maximum intensity (given in the red text). Grids farthest east in the basin tend to have very low observed maximum intensities but relatively higher simulated maximum intensities, although it is generally the case that the per hexagon simulated maximum wind speed is slightly higher than the per hexagon observed maximum wind speed. For example, compare the two eastern most grids. For observed TCs, the maximum intensities observed are 55 and 34 m $s^{-1}$. For the set of simulated TCs, however, the maximum intensities in these grids are 65 and 60 m $s^{-1}$. Because the simulated storms represent a long-term climatology, there is more opportunity to see a very high intensity TC.

[18] Figure 3 illustrates the relative risk of a simulated TC relative to observations. The per hexagon relative risk value is obtained by first calculating the ratio of the per hexagon observed storm counts to the total observed storm count, and similarly for the simulated data. The values shown in Figure 3 are then found by dividing the simulated ratio by the observed ratio for each grid. Hexagons shaded in blue represent a higher risk of a simulated TC relative to the best-track data. This is a means of showing the factor by which simulated TCs exceed observed TCs across the lattice. Again, it is evident that the largest differences occur in the far eastern portion of the basin, where observed storms exceed simulated storms. On the other hand, simulated TCs over the Caribbean tend to exceed observed TCs by a factor of approximately 1.5. Besides these two areas, relatively more synthetic storms appear at higher latitudes. This may be a result of conventions by which observed storms are usually declared extratropical by the time they reach these high latitudes. Consequently, observed storms falling into this category are not included in our analysis, which might lead to a low count relative to the synthetic data.

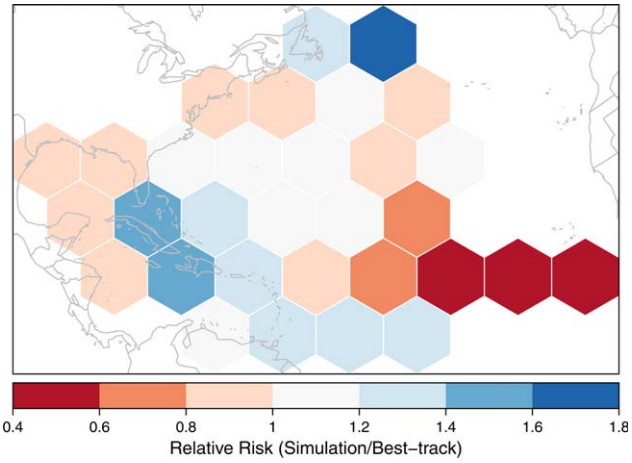


**Figure 3.** Factor by which synthetic tropical cyclone relative frequency exceeds observed relative frequency. Values greater than one (blues) indicate that simulated storm frequency exceeds observed storm frequency, while values less than one (reds) indicate that observed storm frequency exceeds simulated storm frequency.

## 4. Relationship to SST

[19] One advantage of the spatial framework is that we are able to locationally match the hurricane data with covariate information. To demonstrate this, we map the SST field using the same grids as before (Figure 4). Each grid contains the seasonal and grid area-averaged SST value. As expected, maximum SST values occur farther south in the basin and in the Caribbean and Gulf of Mexico. Average ASO SST values generally exceed 27°C in these areas.

[20] We next compute the correlation between per grid average SST values and hurricane counts across the domain for both best-track and simulated data. The correlation between the observed hurricane frequency

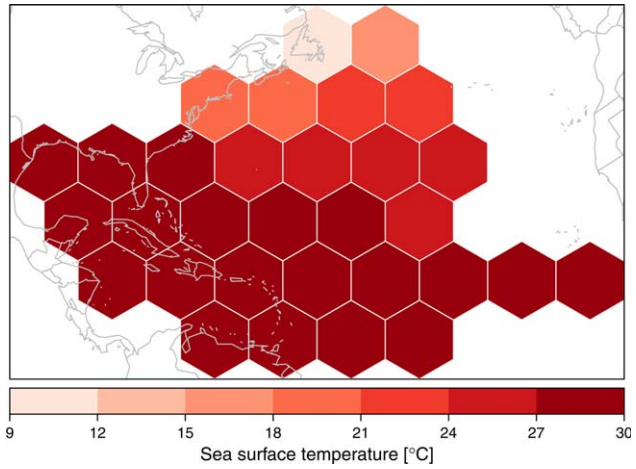


**Figure 4.** August to October sea surface temperature (1980–2010). The raw values are averaged within each hexagon.

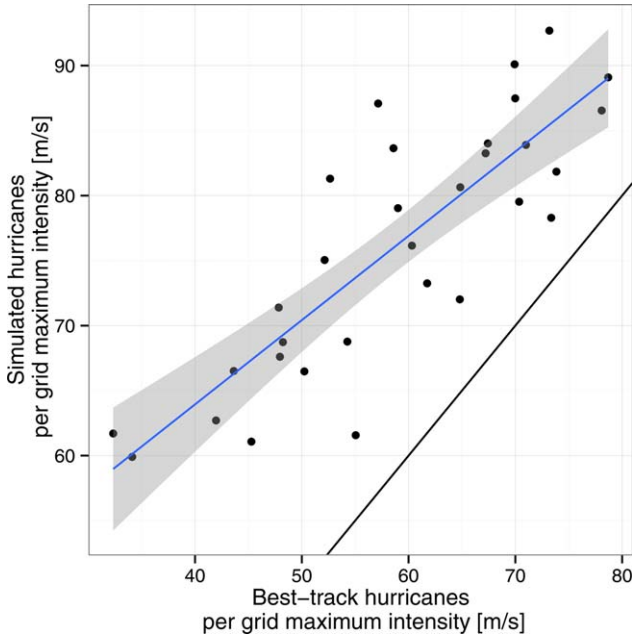


**Figure 5.** Scatterplot of per hexagon maximum intensities (m $s^{-1}$) with observed and synthetic wind speeds given on the abscissa and ordinate axes, respectively. The blue line depicts a linear least-squares fit with 95% confidence interval (gray shading). The black line represents a line through the origin with a slope of one.

and average ASO SST across the domain is +0.27 (−0.10, +0.58) (95% confidence interval, CI). This compares to a correlation of +0.20 (−0.17, +0.52) (95% CI) between the simulated hurricane frequency and SST. If we compare only those values for hexagons with average SST greater than or equal to 25°C, the correlations remain near zero for both observational and synthetic data. Thus, we do not find significant positive correlation between SST and TC frequency. Although warm SSTs are a known necessary condition for TC formation, it is well understood that SST is a poor indicator of genesis. For example, *Goldenberg et al.* [2001] cite vertical shear of the horizontal wind to be the more important local factor affecting TC frequency over the North Atlantic basin. In this respect, the synthetic data match observations quite well. As with the best-track TCs, the frequency of synthetic TCs does not appear to increase with increasing SST.

[21] Correlations are also computed between SST and per grid maximum wind speed. Across all hexagons, the correlation between per grid observed maximum wind speed is +0.66 (+0.39, +0.82) (95% CI). For the synthetic data, this correlation is +0.59 (+0.29, +0.78) (95% CI). Unlike frequency, maximum wind speed is significantly related to grid-averaged ASO SST. These correlations remain approximately the same if we consider only those grids with SST > 25°C to calculate the correlations. Additionally, we calculate the correlation between the best-track and simulated maximum TC intensities. The best-track and simulated maximum hurricane intensities match very well with a correlation of +0.84. This relationship between observed and synthetic maximum wind speed is shown in Figure 5.

[22] High values of correlation suggest a tight relationship between SST and limiting intensity. Limiting intensity (LI), as derived through the statistical model presented in *Elsner et al.* [2012b], describes the theoretical maximum TC intensity based on historical track data. If we regress LI onto SST for each grid, we obtain an estimate of the sensitivity of hurricane limiting intensity to SST. Although the correlations between SST and per grid maximum wind speed hint at a high sensitivity, correlation does not adequately answer the sensitivity question.

[23] To determine the sensitivity values, we first determine the limiting intensities. In *Elsner et al.* [2012b, 2013], LI was estimated from per hurricane maximum wind speeds using a statistical model combining the Generalized Pareto distribution (GPD) for hurricane intensities above a threshold and a Poisson distribution for the frequency of hurricanes exceeding the threshold. The model applied is characterized by scale ($\sigma$) and shape ($\xi$) parameters. The model also relies on the threshold intensity parameter ($u$). The scale parameter, $\sigma$, describes how quickly probabilities decrease away from the threshold value, and $\xi$ describes the length of the tail of the distribution. Only those wind speeds that exceed the threshold value are considered in the model. For $\xi < 0$, the probability decreases to zero beyond a certain wind speed, providing us with a limiting intensity. Additional theory and explanation for this method can be found in *Coles* [2001] and *Jagger and Elsner* [2006].

[24] For $\xi < 0$, we thus estimate the LI from our model to be:

$$\mathrm{LI} = u - \sigma/\xi \tag{1}$$

[25] The scale and shape parameters in equation (1) are determined by the method of maximum likelihood. Using a wind speed threshold of 30 m $s^{-1}$, we estimate

the model from per TC maximum intensity for each hexagon containing at least 21 TCs. Once we have a set of limiting intensities, we then calculate the sensitivity using a linear regression model. Because not all grids have the same number of hurricanes, we use a weighted regression so that those grids with more hurricanes contribute more to the relationship than do those with fewer hurricanes. For the regression, we only consider grids with an average SST of at least 25°C since we are primarily interested in TCs in a more favorable thermodynamic environment and are not interested in higher latitude systems that may be influenced by baroclinic effects. Using this method, we obtain a basin wide sensitivity of $6.3 \pm 2.42$ m $s^{-1}$ $K^{-1}$ (SE) for observed TCs. As expected, this value compares well with the value of 7.9 m $s^{-1}$ $K^{-1}$ obtained by *Elsner et al.* [2012b] who used the period 1981–2010 and considered all TCs, whereas we only consider those with a lifetime maximum wind speed of at least 40 knots.

[26] Although the statistical model allows us to obtain the LI for a set of per hurricane maximum intensities, it comes with the drawback of having to select a threshold value. If the threshold value is set too low, bias increases because the model includes wind speeds that do not represent the strongest TCs. Conversely, if the threshold is set too high, there are not enough wind speeds to reliably estimate the other model parameters [*Coles*, 2001]. There are several techniques that can be used to determine the most appropriate threshold [*Coles*, 2001], but these methods may be far from ideal in many instances and often require some degree of subjective monitoring.

[27] To avoid this complication, we simply choose the per hexagon maximum wind speeds as the LI. In this case, we examine only the maximum wind speed over the area covered by a given hexagon during the 1980–2010 period. Because we are only interested in TCs in nearly optimal thermodynamic conditions, we again only consider hexagons with SST > 25°C. Using this technique, we obtain a sensitivity estimate of $8.6 \pm 1.57$ m/s/K (SE) for observations and $5.5 \pm 1.31$ m/s/K (SE) for the synthetic data. If we take the error into consideration, this compares reasonably well with the previous estimate. In fact, for 15 of the 31 hexagons, the LI estimate from the statistical model is the same as the per hexagon maximum wind speed, indicating that the model may be slightly underestimating the limiting intensity. Keeping this slight bias in mind, we use limiting intensity estimates obtained from per hexagon maximum wind speed rather than those from the GPD-Poisson model for the remainder of the paper.

[28] The weighted linear regressions of LI (determined from per hexagon maximum wind speed and weighted by per hexagon cyclone counts) onto SST are plotted for best-track and synthetic data in Figure 6. Although the synthetic data sensitivity estimate is slightly lower than that for observations, the value is still much higher than most sensitivity values obtained from GCM-generated track data [*Elsner et al.*, 2013]. Intensity estimates for the synthetic data are generated from a very high-resolution deterministic coupled ocean-atmospheric model. Although a simple model, it is better able to resolve eyewall structure and maximum wind speed, as evidenced by the high maximum wind speed values in Figure 2. As hypothesized, sensitivity values for the synthetic data better match observations. From Figure 6, the largest residual for the best-track linear model has a limiting intensity < 40 m $s^{-1}$. This residual occurs in grid 22, which is in the southeast corner of the domain (Figure 2) and will be discussed again in section 5.

[29] These results come from the specific spatial lattice of hexagons introduced in section 3. The results

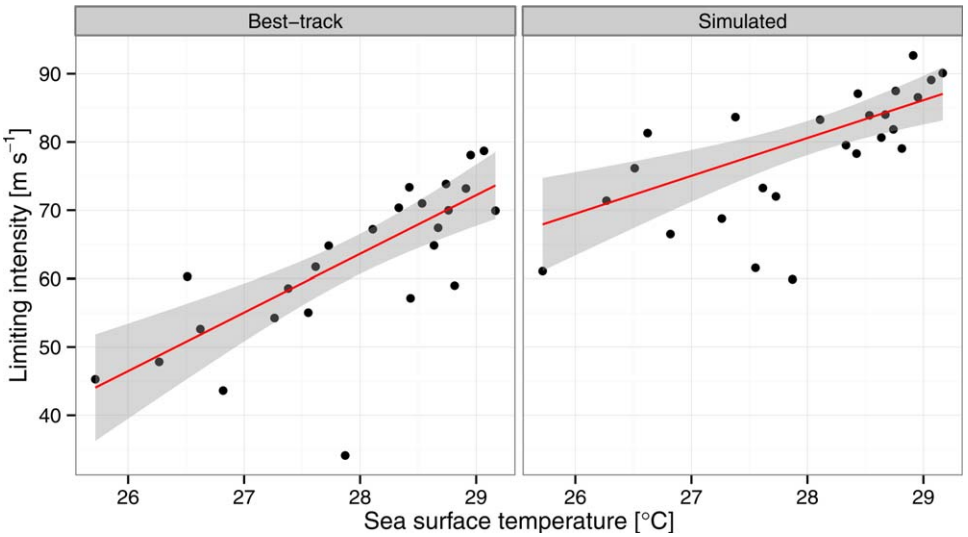


**Figure 6.** Linear regression of per hexagon limiting intensity onto SST for (left) observed and (right) synthetic data. The points represent the data while the red line provides the model fit with 95% confidence intervals depicted by the gray shading. The linear regression model is weighted by the number of tropical cyclones in each hexagon. The slope is an estimate of basin wide sensitivity of limiting intensity to SST.

should remain roughly the same for lattices of larger or smaller hexagons. We test the sensitivity values for four different spatial lattices with hexagons of varying areas both larger and smaller than those used in the previous analysis. The results are presented in Table 1. In general, the basin wide sensitivity estimates from varying grid sizes generally remain stationary with overlapping standard errors for sensitivity among the various grids.

## 5. Regional Patterns of Sensitivity

[30] The sensitivity estimate given above represents an average value over the entire basin. We are also interested in regional patterns of sensitivity. For this section, we again focus on grids with SST $> 25°C$ and estimate sensitivity using LI values defined by per hexagon maximum wind speed. To examine the spatial variability of sensitivity, we begin by calculating the spatial autocorrelation of the linear model residuals using Moran's I [*Moran*, 1950]. The calculated values of Moran's I are 0.25 and 0.52 for best-track and synthetic residuals, respectively. *P*-values of 0.0078 (observations) and $< 0.001$ (synthetic) indicate significant nonzero spatial autocorrelation.

[31] Next, we perform a geographically weighted regression (GWR) of LI onto SST for both the observed and synthetic data sets. The GWR is performed using the same spatial lattice and a bandwidth that minimizes the root mean square prediction error. As before, this regression is also weighted by the number of TCs in each hexagon. The regression coefficient on the SST term indicating regional sensitivity is mapped in Figure 7. The highest sensitivity values are noted over the western part of the basin. We find the lowest sensitivities for both observed and synthetic data occur in the eastern most hexagons. This may be due to edge effects, but also may be related to the very low LI for this particular hexagon. For observations, this hexagon is also the largest residual from Figure 6 and represents an area over which one or two storms may form annually, but where few hurricanes reach their maximum intensity.

[32] Although the basin-averaged sensitivity values for best-track and synthetic data match reasonably well, the spatial variability of this sensitivity appears to be somewhat different. With the exception of higher latitudes, sensitivities for the synthetic storms are generally higher than for observations. This makes sense given the higher synthetic TC wind speeds over lower latitudes compared to observations (see Figure 2). Conversely, synthetic TC sensitivities are lower over higher latitudes compared to observations. For observed storms (see Figure 8), sensitivity values generally increase from east to west. However, for the simulated cases the pattern is not as coherent, with high values over the southern portion of the basin and the Gulf of

**Table 1.** Sensitivity of Limiting Hurricane Intensity to Sea Surface Temperature[a]

| Hexagon Size (Area) $10^5$ km$^2$ | Sensitivity (Observed Data) m s$^{-1}$ K$^{-1}$ | Sensitivity (Synthetic Data) m s$^{-1}$ K$^{-1}$ |
|---|---|---|
| 16.7 | 7.7 ± 2.52 | 7.0 ± 1.93 |
| 11.1 | 9.7 ± 3.21 | 11 ± 2.09 |
| 8.33 | 8.6 ± 1.57 | 5.5 ± 1.31 |
| 5.00 | 7.8 ± 1.55 | 7.1 ± 1.55 |
| 4.17 | 8.1 ± 1.34 | 6.3 ± 1.41 |

[a]Uncertainties are given by standard errors.

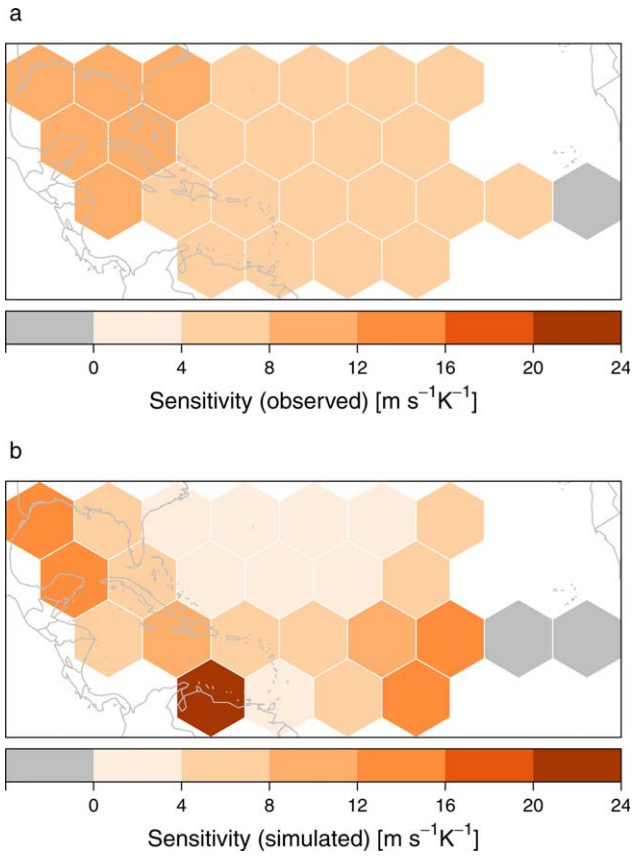


**Figure 7.** Regional estimates of the sensitivity of limiting intensity to SST. The estimates are from a geographically weighted regression of per hexagon limiting intensity onto per hexagon average SST for (a) observed and (b) synthetic data. Hexagons with negative sensitivity are shaded gray.

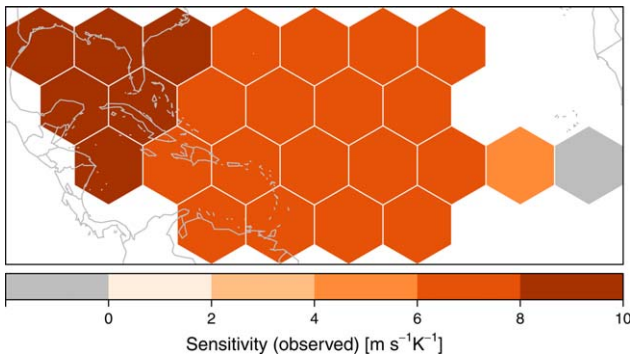


**Figure 8.** Same as Figure 7a except with a different color scale to highlight intrabasin variability in sensitivity computed using the observed (best-track) data.

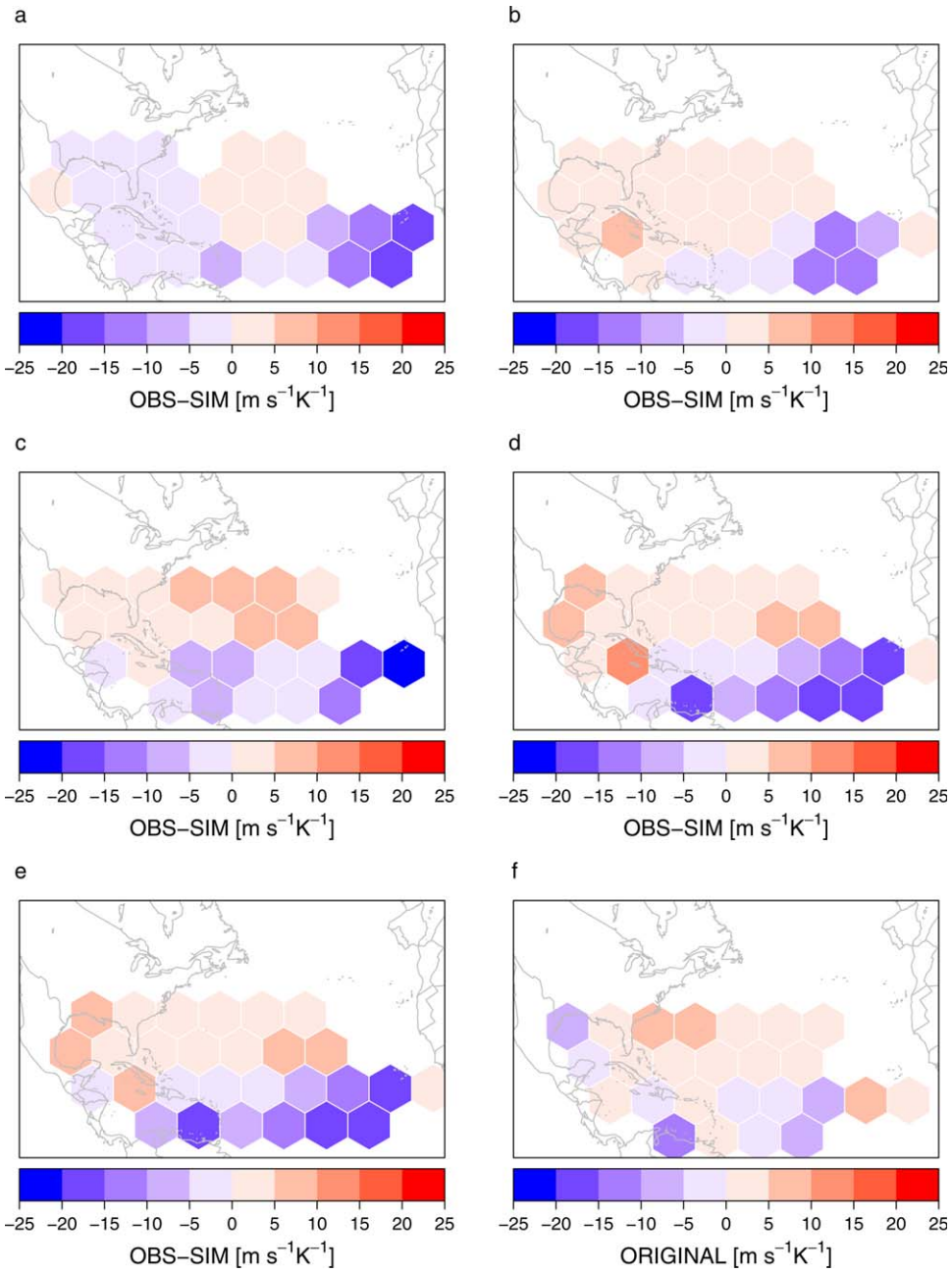


**Figure 9.** Regional differences in the sensitivity of limiting intensity: (a–e) different grids shifted very slightly in space and (f) the original grid from the previous analysis. Blues indicate regions of higher sensitivities for synthetic tropical cyclones and reds indicate regions of higher sensitivities for observed tropical cyclones.

Mexico and lower values along the U.S. eastern seaboard. The higher synthetic sensitivities farther south and east in the basin suggest that the simulated storms may intensify more rapidly.

[33] We set all negative sensitivities to zero and compare the differences in regional sensitivity for observed and synthetic data in Figure 9f. Further, we generate five additional tessellations each slightly offset in space from the original. The offset lattices are displayed in Figures 9a–9e. Blues indicate areas with higher simulated sensitivities, while reds indicate areas with higher observed sensitivities. Although there are some differences among the different grids, the overall pattern suggests that simulated sensitivities are generally higher than observations in the eastern portion of the basin, while best-track sensitivities are higher in the western and northern portions of the basin.

## 6. Summary and Conclusions

[34] A method for simulating hurricanes that makes use of reanalysis data from NCEP and empirical models

has recently been developed. Here we analyze a set of these synthetic hurricanes and compare them to the set of observed hurricanes over the common period 1980–2010. We specifically focus on spatial comparisons of the frequency, intensity, and sensitivity to SST using a hexagon grid covering the North Atlantic basin including the Gulf of Mexico and parts of the Caribbean Sea.

[35] The main findings are:

[36] 1. With a pattern correlation of 0.715, the spatial distribution of TC frequency in the synthetic TC data matches the spatial distribution of the TC frequency in the best-track data. Regions where TCs actually occur generally correlate well with regions where the synthetic TCs are found.

[37] 2. The spatial distribution of TC intensity in the synthetic TC data also matches the spatial distribution of TC intensity in the best-track data. Regions where strong hurricanes occur in the best-track data compare well with regions where strong hurricanes occur in the simulated data.

[38] 3. On average, the sensitivity of limiting intensity to SST is larger in actual hurricanes. The sensitivity is estimated to be 8.6 m $s^{-1}/K^{-1}$ using the best-track data and 5.5 m $s^{-1}/K^{-1}$ using the simulated TCs. This marks an improvement over track data obtained from two climate models with grid spacing of 50 and 100 km [*Elsner et al*., 2013].

[39] 4. The spatial distribution of the occurrence of hurricanes in the simulated set does not match the spatial distribution of the occurrence of hurricanes in the best-track set. In general, sensitivities for simulated storms tend to be higher farther east in the basin compared to observations.

[40] We have shown that several TC statistics for data obtained through the downscaling approach of *Emanuel* [2006] generally agree with observations for the North Atlantic basin. Specifically, the synthetic TCs exhibit a basin wide sensitivity of limiting intensity to SST that is much closer to the observed sensitivity compared to estimates presented in *Elsner et al*. [2013] for two GCMs. This seems reasonable, as intensities for the synthetic tracks were generated using a very high-resolution deterministic model that, unlike coarser resolution climate models, is able to resolve the hurricane eyewall. Despite the improvement, the spatial patterns of sensitivity within the basin for synthetic and best-track data do not agree as well, with higher observed sensitivities farther west and north in the basin, and higher simulated sensitivities farther south and east.

[41] We acknowledge that while SST is an important variable for explaining hurricane LI, other factors influence the intensity TCs can reach. For example, potential intensity [*Emanuel*, 1986; *Bister and Emanuel*, 1998] is greatly influenced by upper tropospheric temperatures [*Emanuel et al*., 2013]. Additionally, environmental factors such as vertical shear of the horizontal wind are known to affect intensity [e.g., *DeMaria*, 1996; *Wang and Chan*, 2004]. Finally, numerous recent studies have addressed the relationship between relative rather than local SSTs and potential intensity [e.g., *Vecchi and Soden*, 2007; *Ramsay and Sobel*, 2011]. Future work will look toward introducing these and other variables into our model. Although we agree that many of these factors indeed may be important, it is nevertheless useful to quantify differences in the sensitivity of LI to SST between simulated and observed TCs. Such quantification provides a metric for assessing model performance in the future as resolution continues to improve.

[42] **Acknowledgment.** Support came from the Risk Prediction Initiative of the Bermuda Institute for Ocean Science (RPI2.0-2012-01).

## References

Bengtsson, L., M. Botzet, and M. Esch (1996), Will greenhouse gas-induced warming over the next 50 years lead to higher frequency and greater intensity of hurricanes?, *Tellus, Ser. A*, *48*, 57–73.

Bister, M., and K. A. Emanuel (1998), Dissipative heating and hurricane intensity, *Meteorol. Atmos. Phys.*, *65*, 233–240.

Broccoli, A. J., and S. Manabe (1990), Can existing climate models be used to study anthropogenic changes in tropical cyclone climate?, *Geophys. Res. Lett.*, *17*, 1917–1920.

Camargo, S. J., A. G. Barnston, and S. E. Zebiak (2005), A statistical assessment of tropical cyclone activity in atmospheric general circulation models, *Tellus, Ser. A*, *57*, 583–604.

Chen, S. S., W. Zhao, M. A. Donelan, J. F. Price, and E. J. Walsh (2007), The CBLAST-Hurricane Program and the next-generation fully coupled atmosphere-wave-ocean models for hurricane research and prediction, *Bull. Am. Meteorol. Soc.*, *88*, 311–317.

Coles, S. (2001), *An Introductiion to Statistical Modeling of Extreme Values*, Springer, London.

DeMaria, M. (1996), The effect of vertical shear on tropical cyclone intensity change, *J. Atmos. Sci.*, *53*, 2076–2088.

Elsner, J. B., and T. H. Jagger (2013), *Hurricane Climatology: A Modern Statistical Guide Using R*, 390 pp., Oxford Univ. Press, New York.

Elsner, J. B., J. P. Kossin, and T. H. Jagger (2008), The increasing intensity of the strongest tropical cyclones, *Nature*, *455*, 92–95.

Elsner, J. B., R. E. Hodges, and T. H. Jagger (2012a), Spatial grids for hurricane climate research, *Clim. Dyn.*, *39*, 21–36.

Elsner, J. B., J. C. Trepanier, S. E. Strazzo, and T. H. Jagger (2012b), Sensitivity of limiting hurricane intensity to ocean warmth, *Geophys. Res. Lett.*, *39*, L17702, doi:10.1029/2012GL053002.

Elsner, J. B., S. E. Strazzo, T. H. Jagger, T. LaRow, and M. Zhao (2013), Sensitivity of limiting hurricane intensity to SST in the Atlantic from observations and GCMs, *J. Clim.*, doi:10.1175/JCLI-D-12–00433.1, in press.

Emanuel, K. (2005), Increasing destructiveness of tropical cyclones over the past 30 years, *Nature*, *436*, 686–688.

Emanuel, K. A. (1986), An air-sea interaction theory for tropical cyclones. Part I: Steady-state maintenance, *J. Atmos. Sci.*, *43*, 585–605.

Emanuel, K. A. (2006), Climate and tropical cyclone activity: A new model downscaling approach, *J. Clim.*, *19*, 4797–4802.

Emanuel, K. A. (2010), Tropical cyclone activity downscaled from NOAA-CIRES reanalysis, 1908–1958, *J. Adv. Model. Earth Syst.*, *2*(1), doi:10.3894/JAMES.2010.2.1.

Emanuel, K., S. Ravela, E. Vivant, and C. Risi (2006), A statistical deterministic approach to hurricane risk assessment, *Bull. Am. Meteorol. Soc.*, *87*(3), 299–314.

Emanuel, K. A., R. Sundararajan, and J. Williams (2008), Hurricanes and global warming: Results from downscaling IPCC AR4 simulations, *Bull. Am. Meteorol. Soc.*, *89*, 347–367.

Emanuel, K. A., S. Solomon, D. Folini, S. Davis, and C. Cagnazzo (2013), Influence of tropical tropopause layer cooling on Atlantic hurricane activity, *J. Clim.*, *26*, 2288–2301.

Goldenberg, S. B., C. W. Landsea, A. M. Mestas-Nuñez, and W. M. Gray (2001), The recent increase in Atlantic hurricane activity: Causes and implications, *Science*, *293*, 474–479.

Jagger, T. H., and J. B. Elsner (2006), Climatology models for extreme hurricane winds near the United States, *J. Clim.*, *19*, 3220–3236.

Jarvinen, B. R., C. J. Neumann, and M. A. S. Davis (1984), A tropical cyclone data tape for the North Atlantic basin, 1886–1983: Contents, limitations and uses, *NOAA Tech. Memo. NWS NHC 22*, 21 pp., Natl. Oceanic and Atmos. Admin., Coral Gables, Fla.

Knutson, T. R., J. L. McBride, J. Chan, K. Emanuel, G. Holland, C. Landsea, I. Held, J. P. Kossin, A. K. Srivastava, and M. Sugi (2010), Tropical cyclones and climate change, *Nat. Geosci.*, *3*, 157–163.

Kossin, J. P., S. J. Camargo, and M. Sitkowski (2010), Climate modulation of North Atlantic hurricane tracks, *J. Clim.*, *23*, 3057–3076.

Landsea, C. W., C. Anderson, N. Charles, G. Clark, J. Dunion, J. Fernandez-Partagas, P. Hungerford, C. Neumann, and M. Zimmer (2004), The Atlantic hurricane database re-analysis project: Documentation for the 1851–1910 alterations and additions to the HURDAT database, in *Hurricanes and Typhoons: Past, Present and Future*, edited by R. I. Murnane and K. B. Liu, pp. 177–221, Columbia Univ. Press, New York.

LaRow, T. E., Y. K. Lim, D. W. Shin, E. P. Chassignet, and S. Cocke (2008), Atlantic basin seasonal hurricane simulations, *J. Clim.*, *21*, 3191–3206.

Mann, M. E., and K. A. Emanuel (2006), Atlantic hurricane trends linked to climate change, *EOS Trans. AGU*, *87*, 233–244, doi:10.1029/2006EO240001.

Moran, P. A. P. (1950), Notes on continuous stochastic phenomena, *Biometrika*, *37*, 17–33.

Murakami, H., B. Wang, and A. Kitoh (2011), Future change of western North Pacific typhoons: Projections by a 20-km-mesh global atmospheric model, *J. Clim.*, *24*, 1154–1169.

Oouchi, K., J. Yoshimura, H. Yoshimura, R. Mizuta, and A. Noda (2006), Tropical cyclone climatology in a global-warming climate as simulated in a 20 km-mesh global atmospheric model: Frequency and wind intensity analyses, *J. Meteorol. Soc. Jpn.*, *84*, 259–276.

Ramsay, H. A., and A. H. Sobel (2011), Effects of relative and absolute sea surface temperature on tropical cyclone potential intensity using a single-column model, *J. Clim.*, *24*, 183–193.

Strazzo, S., J. B. Elsner, T. LaRow, D. J. Halperin, and M. Zhao (2013), Observed versus GCM-generated local tropical cyclone frequency: Comparisons using a spatial lattice, *J. Clim.*, doi: 10.1175/JCLI-D-12-00808.1.

Vecchi, G., and B. Soden (2007), Effect of remote sea surface temperature change on tropical cyclone potential intensity, *Nature*, *450*, 1066–1071.

Vecchi, G., K. Swanson, and B. Soden (2008), Whither hurricane activity, *Science*, *322*, 687–689.

Wang, M. L. M., and J. C. L. Chan (2004), Tropical cyclone intensity in vertical wind shear, *J. Atmos. Sci.*, *61*, 1859–1876.

Zhao, M., I. M. Held, S. J. Lin, and G. A. Vecchi (2009), Simulations of global hurricane climatology, interannual variability, and response to global warming using a 50-km resolution GCM, *J. Clim.*, *22*, 6653–6678.

Corresponding author: S. Strazzo, Department of Geography, Florida State University, Tallahassee, FL 32306-2190, USA. (ses09e@fsu.edu)